BIOCHEMISTRY
including biophysical chemistry & molecular biology

ARTICLE

pubs.acs.org/biochemistry

# Shear Flow Induced Changes in Apolipoprotein C-II Conformation and Amyloid Fibril Formation

Chai Lean Teoh,[†] Innocent B. Bekard,[‡] Peter Asimakis,[‡] Michael D. W. Griffin,[†] Timothy M. Ryan,[†] Dave E. Dunstan,[*,‡] and Geoffrey J. Howlett[†]

[†]Department of Biochemistry and Molecular Biology, Bio21 Molecular Science and Biotechnology Institute, The University of Melbourne, Parkville, Victoria 3010, Australia

[‡]Department of Chemical and Biomolecular Engineering, The University of Melbourne, Parkville, Victoria 3010, Australia

**ABSTRACT:** The misfolding and self-assembly of proteins into amyloid fibrils that occur in several debilitating diseases are affected by a variety of environmental factors, including mechanical factors associated with shear flow. We examined the effects of shear flow on amyloid fibril formation by human apolipoprotein C-II (apoC-II). Shear fields (150, 300, and 500 $s^{-1}$) accelerated the rate of apoC-II fibril formation (1 mg/mL) approximately 5−10-fold. Fibrils produced at shear rates of 150 and 300 $s^{-1}$ were similar to the twisted ribbon fibrils formed in the absence of shear, while at 500 $s^{-1}$, tangled ropelike structures were observed. The mechanism of the shear-induced acceleration of amyloid fibril formation was investigated at low apoC-II concentrations (50 $\mu$g/mL) where fibril formation does not occur. Circular dichroism and tryptophan fluorescence indicated that shear induced an irreversible change in apoC-II secondary structure. Fluorescence resonance energy transfer experiments using the single tryptophan residue in apoC-II as the donor and covalently attached acceptors showed that shear flow increased the distance between the donor and acceptor molecules. Shear-induced higher-order oligomeric species were identified by sedimentation velocity experiments using fluorescence detection, while fibril seeding experiments showed that species formed during shear flow are on the fibril formation pathway. These studies suggest that physiological shear flow conditions and conditions experienced during protein manufacturing can exert significant effects on protein conformation, leading to protein misfolding, aggregation, and amyloid fibril formation.

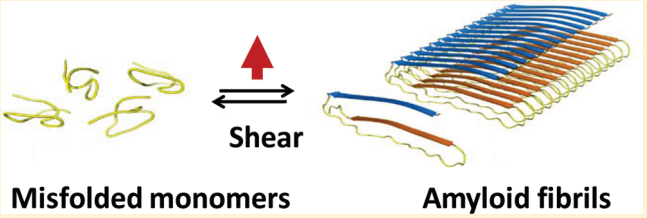


Amyloid fibrils are formed by the self-assembly of a range of naturally occurring proteins that misfold and aggregate into structures that share a number of common properties. The defining characteristics of amyloid fibrils include cross-$\beta$ structure and the ability to interact with the dyes thioflavin T (ThT) and Congo Red.[1] Of the more than 25 proteins known to self-assemble into amyloid fibrils in vivo, there is little shared similarity of primary sequence or homology of native structure.[2,3] Several studies indicate that partial unfolding of native proteins is a prerequisite for aggregation and amyloid fibril formation.[4−6] Several factors within amyloid plaques exert effects on fibril formation, including the presence of lipids or lipid complexes, metal ions, glycosaminoglycans, and proteins.[7] Other environmental conditions associated with protein misfolding and aggregation include changes in temperature,[8] ionic strength,[9] pH,[10,11] and exposure to interfaces[12,13] and oxidative agents.[14−16] Considerable anecdotal evidence also suggests mechanical effects and shear flow can affect amyloid fibril formation. Stirring, shaking, mechanical agitation,[17−19] and other shear-inducing conditions such as ultrasonication[20] and ultrafiltration[21] can affect amyloid fibril formation. In addition, differences in fibril morphologies for fibrils grown under quiescent compared to agitated conditions have been observed for amyloid-$\beta$ fibrils[22,23] and fibrils composed of a pathogenic PrP fragment.[23]

High-shear fields are encountered in the body where intravascular fluids are continuously subjected to mechanical shear forces caused by the pulsatile nature of blood flow. Shear flow is also an important factor in the biopharmaceutical industry during processing of protein-based therapeutics. Hemodynamic factors have an initiating role, or at least a potentiating role, in atherosclerosis,[24] raising the possibility that shear flow could influence plaque development via a direct effect on protein folding and aggregation. Recent reports indicate that up to 60% of atherosclerotic lesions contain fibrillar proteins.[25,26] Of the proteins known to misfold and aggregate in vivo, apolipoproteins (apo) B100, A-I, A-II, A-IV, and E and serum amyloid A are prevalent in atherosclerotic lesions.[27] While these proteins are normally present in vivo in lipid-rich lipoproteins, under lipid-poor conditions in vitro, several of these proteins readily assemble into amyloid fibrils.[28,29] The deposition of misfolded proteins in the arterial wall may contribute to the reduced elasticity of the blood vessels and the initiation of vascular inflammation and atherosclerosis.

One of the components of very low-density lipoproteins, and a key cofactor for lipoprotein lipase, human apoC-II (8.9 kDa) is a

**Received:** February 17, 2011
**Revised:** April 5, 2011
**Published:** April 09, 2011

small protein composed of 79 amino acids with only a single tryptophan residue and no cysteine or histidine residues. In vitro studies show that, in common with other lipoproteins, apoC-II has low conformational stability in a lipid-free environment and readily aggregates, without the need for agitation, into homogeneous fibrils with all the characteristics of amyloid.[30−32] This includes the ability to bind the dyes ThT and Congo Red, the presence of cross-$\beta$ structure, and the ability to associate with nonfibrillar components of amyloid deposits, which includes serum amyloid P (SAP) and apoE.[33,34] Immunohistochemistry of human coronary artery plaques shows colocalization of apoC-II with SAP, a universal marker for amyloid deposits.[35] ApoC-II fibrils, along with A$\beta$ fibrils, activate macrophage inflammatory responses via the CD36 receptor, leading to an increase in the rate of production of reactive oxygen species.[36] Activation of macrophages is associated with foam cell formation, an early event in the development of atherosclerosis, suggesting that apolipoprotein amyloid fibril formation and deposition in the artery walls may be linked to disease.

Molecular level conformational changes in proteins due to applied stress were first shown by Astbury and co-workers,[37] leading to a number of theoretical and experimental investigations.[38−42] Experimental studies on protein systems in this field give conflicting reports. Early reports showed that fluid forces significantly impair the catalytic activity of several enzymes after exposure to shear rates as low as $\sim$10 $s^{-1}$,[38] while later investigations found little or no evidence of shear deactivation of these enzymes at higher shear rates.[42] For this reason, it was postulated that enzyme denaturation observed in earlier studies may be a consequence of air−liquid interface interaction and not shear. However, later studies, in which more sensitive structural techniques such as real-time fluorescence spectroscopy were used to directly monitor the shear stability of horse cytochrome *c*,[40] and human von Willebrand factor (vWF)[43] under hydrodynamic shear stress in capillary flow, also gave conflicting results. While cytochrome *c* showed no structural changes for shear rates as high as $10^5$ $s^{-1}$, vWF demonstrated structural instability at a threshold shear rate of $10^3$ $s^{-1}$. Nonetheless, a study of the effect of simple shear on the helix−coil transition of poly-L-lysine (PLL) provided convincing evidence that simple shear can influence the unfolding equilibrium in a polypeptide.[44] More recently, $\alpha$-helical PLL was revealed to unfold in simple shear flow, with the extent of unfolding shown to be dependent on chain length, as well as the shear rate and the duration of its application.[45]

Earlier reports on the effects of shear flow on amyloid fibril formation have used poorly controlled shear conditions, in which the velocity gradients were heterogeneous, in both space and time, such that the rates, nature, and duration of shear exposure could not be accurately specified.[17−23] In this study, a Couette flow cell was used to generate a well-defined shear field. The device incorporates an optical path that allows continuous spectrophotometric monitoring of the solution conformation of protein samples during shear flow.[46] This permitted a real-time assessment of the effect of shear on apoC-II conformation and amyloid fibril formation. We show that shear accelerates the rate of apoC-II fibril formation. Evidence of the intermolecular association of denatured monomers is presented, which gives rise to an on-pathway prefibrillar oligomeric species that nucleates apoC-II fibril assembly and reduces the time required for fibril development.

## MATERIALS AND METHODS

**Materials.** BL21(DE3) *Escherichia coli* competent cells were purchased from Invitrogen. Forward and reverse oligonucleotide primers encoding mutations for the generation of apoC-II mutants were purchased from GeneWorks. Thioflavin T (ThT) and 5-({2-[(iodoacetyl)amino]ethyl}amino)naphthalene-1-sulfonic acid (1,5-I-AEDANS) were purchased from Sigma (St. Louis, MO), whereas Alexa488 $C_5$ maleimide was obtained from Invitrogen.

**Mutagenesis, Expression, and Purification of ApoC-II.** Wild-type and mutant apoC-II were expressed in *E. coli* BL21-(DE3) cell lines transformed with the pET-11a expression vector containing human apoC-II cDNA. All mutants (S11C, V45C, and W26F/Y37W/S61C) were constructed using the QuickChange method according to the manufacturer's protocol (Stratagene, La Jolla, CA), and multiple rounds of QuickChange mutagenesis were performed if necessary to construct multiple mutations. Mutations in the apoC-II gene were verified by DNA sequencing (Applied Diagnostics, Victoria, Australia). The mutated DNA was isolated and purified by Miniprep (Qiagen Inc.) and then transformed into *E. coli* BL21(DE3) cells for expression and purification as described previously.[30] The molecular masses of wild-type and mutant apoC-II preparations were confirmed on a QTOF LC mass spectrometer (Agilent Technologies Inc.). Purified apoC-II preparations were stored as 30−40 mg/mL stocks at −20 °C in 5 M GuHCl and 10 mM Tris-HCl (pH 8.0) and in the presence of 5 mM TCEP for cysteine substitution mutants.

**Fluorescence Labeling of ApoC-II Cysteine Derivatives.** For a typical 1,5-I-AEDANS labeling reaction, apoC-II cysteine mutant stock solutions of 1.0−1.2 mg/mL were incubated with 5 mM DTT at room temperature for 1−2 h. At 4 °C, the treated samples were passed through NAP-5 desalting columns (GE Healthcare-Amersham Biosciences, Piscataway, NJ) pre-equilibrated in 100 mM sodium phosphate (pH 7.0), previously purged with nitrogen gas. A 20-fold molar excess of 1,5-I-AEDANS was immediately added to the eluted protein from a freshly prepared stock solution of 40 mM 1,5-I-AEDANS prepared in dimethyl sulfoxide. The mixtures were incubated in darkness overnight at 4 °C. Free 1,5-I-AEDANS was removed by applying the protein mixtures to NAP-5 columns pre-equilibrated in 5 M GuHCl and 50 mM Tris-HCl (pH 7.0) at room temperature and further dialyzed against the same buffer over 3 days, with three buffer changes. The preparations were then concentrated using a Centricon Ultracel YM-3 centrifugal filter device (Millipore). ApoC-$II_{S11C}$ was conjugated with Alexa dye, as described by the product manual. Briefly, the sample was incubated with a 3-fold molar excess of Alexa488 $C_5$ maleimide for 90 min at room temperature. Free Alexa maleimide was removed by gel filtration with a G25 Sephadex column (GE Healthcare-Amersham Biosciences). The labeling efficiency was determined spectrophotometrically, assuming molar extinction coefficients for 1,5-I-AEDANS at 336 nm of 5700 $M^{-1}$ $cm^{-1}$, for Alexa488 at 495 nm of 71000 $M^{-1}$ $cm^{-1}$, and for apoC-II at 280 nm of 11000 $M^{-1}$ $cm^{-1}$. Labeling efficiencies were typically 80−95%. The labeling specificities of the protein preparations were confirmed on a Q-TOF LC mass spectrometer (Agilent Technologies Inc.). Labeled samples were stored as 1−1.8 mg/mL stocks in 5 M GuHCl and 50 mM Tris-HCl (pH 7.0) at −20 °C.

**ApoC-II Sample Preparation.** To study the effects of shear on the amyloid fibril forming properties of apoC-II, the protein was refolded by dilution to 1 mg/mL from a denaturing stock

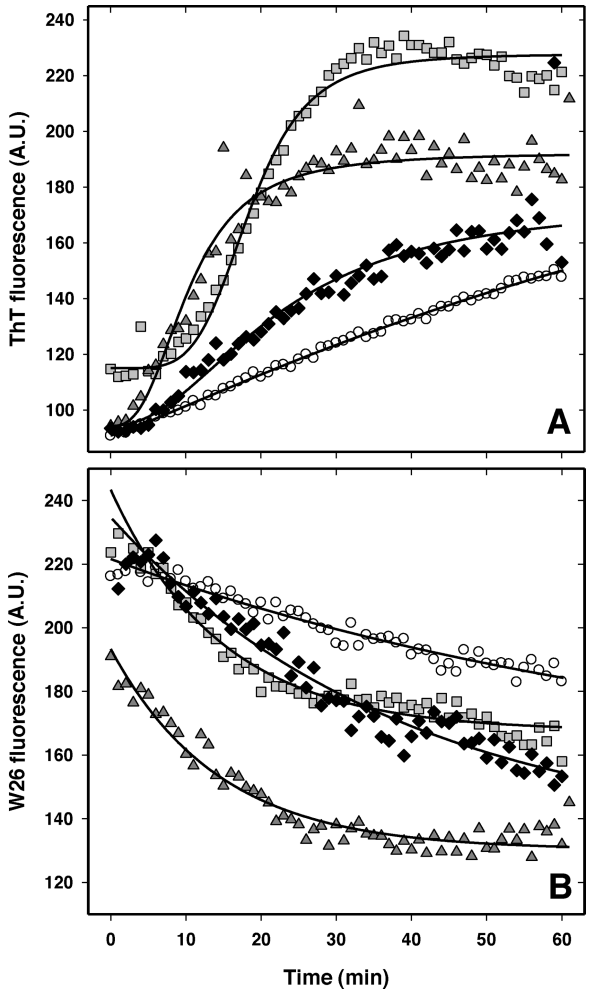


**Figure 1.** Amyloid fibril formation by apoC-II in the absence and presence of shear. ApoC-II (1 mg/mL in refolding buffer containing 55 $\mu$M ThT) was freshly prepared and incubated at room temperature without shear (0 $s^{-1}$) (○) or sheared at rates of 150 $s^{-1}$ (gray squares), 300 $s^{-1}$ (dark gray triangles), and 500 $s^{-1}$ (◆). Amyloid fibril formation was monitored by the changes in ThT fluorescence (A). Effects of varying the shear rates on intrinsic tryptophan fluorescence were also monitored (B).

solution into refolding buffer [100 mM sodium phosphate and 0.1% sodium azide (pH 7.4)] containing 55 $\mu$M ThT. For other studies, 0.1 mg/mL apoC-II preparations in 5 M GuHCl were refolded using a NAP-5 desalting column (GE Healthcare-Amersham Biosciences) pre-equilibrated in 50 mM Tris-HCl, 50 mM NaCl, 2 mM TCEP, and 0.1% sodium azide. When the protein was eluted, its final concentration was adjusted to 50 $\mu$g/mL. Under such conditions, the formation of fibrils by apoC-II is not detectable.[47]

**Controlled Shear.** Shear experiments were performed in a custom-built Couette cell, as previously described.[46,48,49] A significant advantage of a narrow gap Couette cell is the ability to expose protein solutions to uniform, well-defined shear rates for controlled periods. The all-quartz Couette cell was mounted and aligned in the sample compartment of a fluorescence spectrometer or a CD spectrometer, allowing continuous measurement during controlled shearing. ApoC-II solutions (1 mg/mL) were exposed to shear rates of 150, 300, and 500 $s^{-1}$ for 1 h,

**Table 1. Summary of the Changes in ThT and W26 Fluorescence Properties of ApoC-II during Amyloid Fibril Formation in the Absence and Presence of Shear**

| | 0 $s^{-1}$ | 150 $s^{-1}$ | 300 $s^{-1}$ | 500 $s^{-1}$ |
|---|---|---|---|---|
| ThT fluorescence | | | | |
| $S_{max}$ (arbitrary units)[a] | 275.67 | 227.79 | 192.33 | 175.00 |
| $t_{50}$ (min)[b] | 115.95 | 18.48 | 10.41 | 22.30 |
| $n$ | 1.14 | 4.77 | 2.70 | 2.12 |
| W26 fluorescence[b] | | | | |
| $F_{max}$ (arbitrary units) | 221.58 | 243.34 | 193.32 | 234.71 |
| $F_{min}$ (arbitrary units) | 150.16 | 167.56 | 130.30 | 133.24 |
| $t_{50}$ (min) | 56.35 | 10.15 | 9.94 | 26.66 |
| $\lambda_{max}$ emission of W26 (nm)[c] | | | | |
| $t$ = 0 min | 346.15 | 344.24 | 344.24 | 346.15 |
| $t$ = 60 min | 345.20 | 337.54 | 336.58 | 343.28 |
| $F_{max}$ emission of W26 (arbitrary units)[c] | | | | |
| $t$ = 0 min | 205.00 | 218.42 | 178.02 | 200.85 |
| $t$ = 60 min | 192.31 | 175.43 | 150.60 | 153.03 |

[a] Values for the maximal change in ThT fluorescence $S_{max}$. $t_{50}$ values and $n$ values were obtained by fitting the data in Figure 1A to a Hill plot (eq 1). [b] Values of $F_{max}$, $F_{min}$, and $t_{50}$ were obtained by fitting the data in Figure 1B assuming a single-exponential decay in which $F_{max}$ and $F_{min}$ are the initial and final fluorescence emission values, respectively, and $t_{50}$ is the time required to reach the half-maximal change in fluorescence. [c] The emission maxima ($\lambda_{max}$) of W26 and maximal W26 fluorescence ($F_{max}$) were obtained from spectra recorded at the beginning and end of the application of shear field (Figure 2).

whereas 50 $\mu$g/mL apoC-II samples, where fibril formation cannot be detected, were subjected to a shear rate of 500 $s^{-1}$ for 5 − 30 min. For subsequent analysis, samples were recovered from the shear cell at the end of the experiments and retained.

**Fluorescence Spectroscopy.** All fluorescence measurements were recorded in a Cary Eclipse fluorescence spectrometer (Varian Inc.). Fibril formation was monitored by measuring ThT emission at 485 nm using an excitation wavelength of 442 nm. ThT time courses were fitted to an empirical Hill equation as described previously[50]

$$S = \frac{S_{max} t^n}{t_{50}{}^n + t^n} \quad (1)$$

where $S$ is the signal intensity, $S_{max}$ is the maximal change in signal, $n$ is a cooperativity factor, $t$ is time, and $t_{50}$ is the time for the half-maximal signal change. Values derived for $t_{50}$ were used to compare the effects of shear on the rate of fibril formation.

Tryptophan emission was recorded at 350 nm or collected over the range of 305−550 nm using an excitation wavelength of 295 nm. The fluorescence emission of 1,5-I-AEDANS-modified apoC-II derivatives was recorded at 490 nm using an excitation wavelength of 336 nm. FRET from tryptophan to covalently attached AEDANS was measured using an excitation wavelength of 295 nm and recording fluorescence emission intensity at 490 nm. All emission measurements were corrected for the light scattering contribution of buffer alone. FRET efficiencies were calculated from the tryptophan emission of the unlabeled and labeled apoC-II derivatives according to eq 2

$$E = 1 - \frac{F_{DA}}{F_D} \quad (2)$$


dx.doi.org/10.1021/bi2002482 |*Biochemistry* 2011, 50, 4046–4057

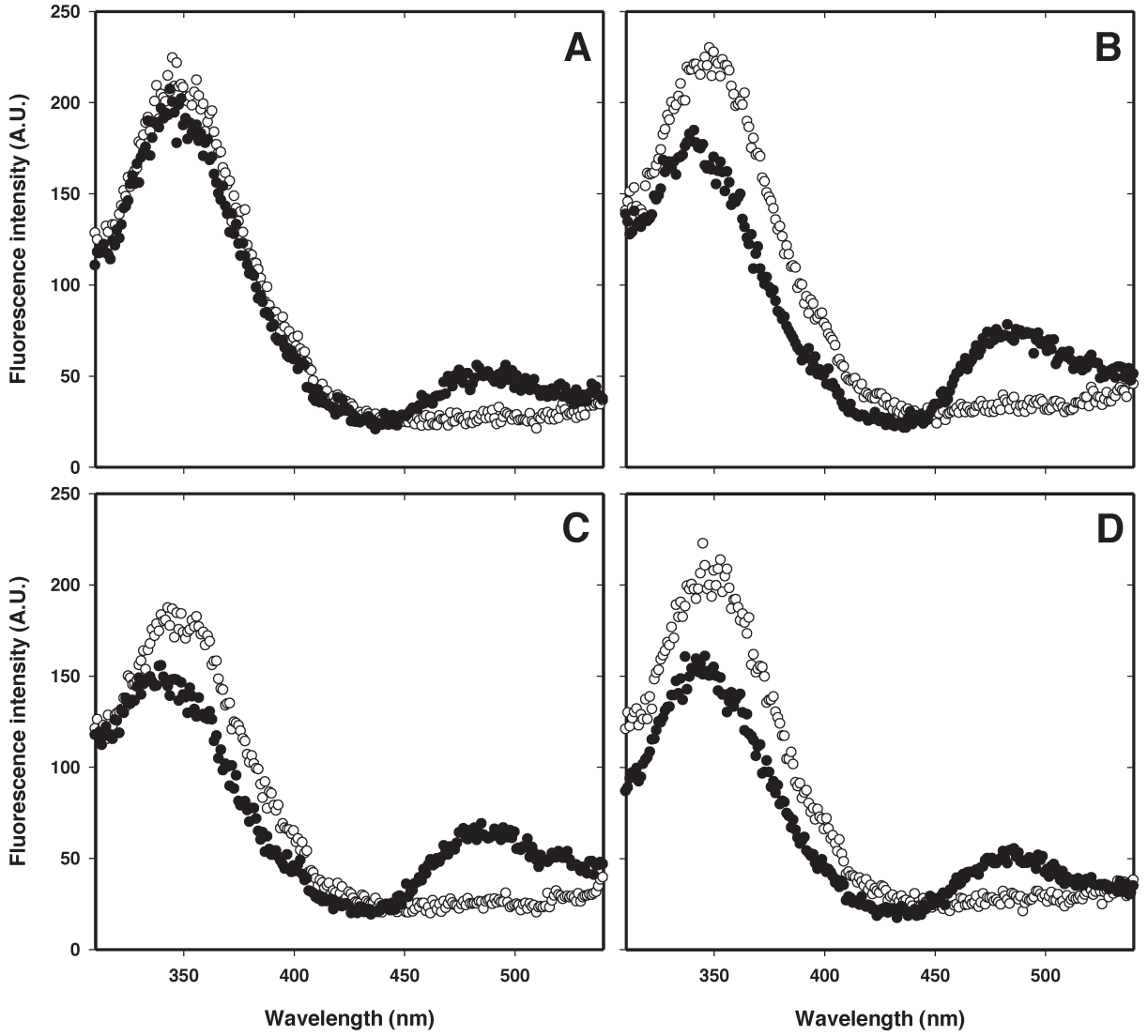


**Figure 2.** Fluorescence emission spectra of apoC-II in the absence and presence of shear. Emission spectra were recorded after excitation at 295 nm for samples (1 mg/mL) freshly refolded (○) and after incubation for 60 min (●) at room temperature: (A) 0, (B) 150, (C) 300, and (D) 500 $s^{-1}$.

where $F_{DA}$ is the fluorescence intensity of the molecule with the donor and acceptor fluorophore attached and $F_D$ is the fluorescence intensity of the molecule with only the donor. The FRET distance $r$ between the donor and acceptor was calculated according to eq 3

$$E = \frac{{R_0}^6}{{R_0}^6 + r^6} \quad (3)$$

where $R_0$ is the Förster radius. A value of 22 Å for $R_0$ was taken for the Trp−AEDANS donor−acceptor pair.[51]

**Transmission Electron Microscopy.** Copper or gold grids (400 mesh) were coated with a thin carbon film and glow discharged in nitrogen. ApoC-II amyloid fibril samples were diluted to a concentration of 0.1 mg/mL with deionized water. The diluted samples were applied to the grids for 1−2 min within 15 min of glow discharging and stained twice with 2% potassium phosphotungstate or uranyl acetate at pH 6.0−7.0. The grids were air-dried and examined using a FEI Tecnai12 microscope operating at 120 kV.

**CD Spectroscopy.** CD measurements were taken at 25 °C using a Jasco (Tokyo, Japan) J-815 CD spectrometer over the wavelength range of 190−240 nm. A spectral bandwidth of 1 nm, a signal average time of 4 s, and a data interval of 0.1 nm were used. The spectra presented were corrected using data obtained for a reference solution lacking apoC-II.

**Sedimentation Analysis.** Sedimentation experiments were conducted using an XL-A analytical ultracentrifuge (Beckman Coulter Instruments, Inc., Fullerton, CA), an An-60Ti rotor, and double-sector 12 mm path length cells containing sapphire windows and charcoal-filled Epon centerpieces. A fluorescence detection system (FDS) (Aviv Associates Inc.) was used to monitor the fluorescence of labeled apoC-II derivatives.[52] Sedimentation velocity data for Alexa488-labeled apoC-II were obtained at 20 °C using a rotor speed of 50000 rpm (201600$g$). FC43 mineral oil (Fluorinert) was added to each sector to move the base of the sample away from the cell bottom.[53] Fluorescence data were collected at 1 min intervals from 6 to 7.0 cm with the excitation laser focused at a spot 20 $\mu$m in diameter, 31 $\mu$m below the surface of the sapphire window. Sedimentation velocity data


dx.doi.org/10.1021/bi2002482 |*Biochemistry* 2011, 50, 4046–4057

were analyzed using the $c(s)$ program SEDFIT 9.4[54] with maximal entropy regularization to convert the experimental data into a continuous size distribution.

**Seeding of Amyloid Fibril Formation.** Freshly refolded apoC-II (50 $\mu$g/mL) was sheared for 30 min at 500 $s^{-1}$ in Couette flow, where fibril formation is negligible. The sample was recovered at the end of shear exposure and then tested as a seed of fibril formation by supplementing this solution with freshly refolded apoC-II at a final protein concentration of 0.3 mg/mL. The proportion of seed to fresh apoC-II is 3.5% (w/w). Development of fibril growth was monitored by taking sample aliquots, in triplicate, at selected time points and determining the change in ThT (5 $\mu$M) fluorescence intensity measured in an *f*max fluorescence plate reader (Molecular Devices, Sunnyvale, CA) equipped with 444 nm excitation and 485 nm emission filters. Control solutions were also measured, where the sheared apoC-II seed was replaced with unsheared apoC-II.

## RESULTS

**Effects of Shear on ApoC-II Amyloid Fibril Formation.** ApoC-II solutions (1 mg/mL) were placed in a Couette flow cell[46,48,49] and subjected to shear rates in the range of 0−500 $s^{-1}$. The time evolution of apoC-II fibril formation, monitored by ThT fluorescence emission, for selected shear rates is shown in Figure 1A. The data show a shear-induced increase in the extent of fibril formation, albeit with a complex dependence on the magnitude of the shear field. The data were fitted empirically to the Hill equation (solid lines) to obtain estimates for the maximal ThT fluorescence, the time ($t_{50}$) to reach half-maximal fibril formation, and the cooperativity factor (Table 1). The $t_{50}$ values for apoC-II amyloid fibrils formed at shear rates of 0, 150, 300, and 500 $s^{-1}$ were estimated to be approximately 131, 18, 10, and 22 min, respectively. The significant decrease in $t_{50}$ values for samples exposed to shear indicates shear enhancement of apoC-II amyloid fibril formation. The application of a shear field also induced changes in the maximal ThT fluorescence and cooperativity factor (Table 1). These changes may be related to changes in the overall morphology of fibrils formed at the different shear rates as revealed by electron microscopy (see below).

For the same samples, a decrease in the emission intensity of the tryptophan residue in apoC-II (W6) was observed during shear exposure (Figure 1B). Previous studies show that W26 fluorescence increases during fibril formation as it becomes more shielded from the aqueous environment.[30] However, when ThT is present, fluorescence resonance energy transfer (FRET) occurs between W26 and fibril-bound ThT, leading to a decrease in W26 fluorescence.[30] This decrease in W26 fluorescence shown in Figure 1B was fitted empirically to a three-parameter exponential decay equation (solid lines) yielding $t_{50}$ values of approximately 56, 10, 10, and 27 for samples subjected to shear rates of 0, 150, 300, and 500 $s^{-1}$, respectively. These data provide further support for shear flow acceleration of apoC-II fibril formation.

Figure 2 shows W26 fluorescence emission spectra for apoC-II samples (1 mg/mL) before and after a 60 min exposure to shear fields of 0, 150, 300, and 500 $s^{-1}$. In the absence of shear, there is very little change in W26 emission over this time period but an increase in emission at approximately 483 nm that can be attributed to FRET from W26 to the fibril-bound ThT.[30] Shearing induces a decrease in the W26 fluorescence emission (Table 1) coupled with an increase in emission at around 483 nm, consistent with FRET with ThT as the acceptor. The magnitude of this FRET effect is greater for the samples subjected to shear flow. In addition, the emission spectra for W26 show blue shifts in wavelength maxima (Table 1), consistent with the formation of fibrils[30] and demonstrating that as fibrils are formed in the presence of shear, W26 moves to a more hydrophobic environment.

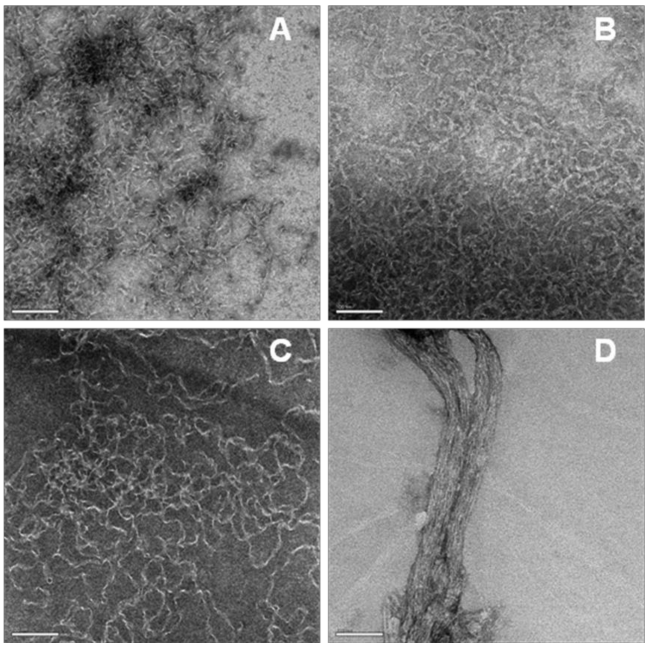


**Figure 3.** Transmission electron micrographs of apoC-II amyloid fibrils formed in the absence and presence of shear. Freshly prepared apoC-II (1 mg/mL in refolding buffer containing 55 $\mu$M ThT) was incubated for 60 min in the absence and presence of shear: (A) 0, (B) 150, (C) 300, and (D) 500 $s^{-1}$. Scale bars for EM images are 100 nm.

**Electron Microscopy Analysis of ApoC-II Amyloid Fibrils.** At the end of a 60 min exposure to shear, samples were recovered from the shear cell and analyzed by transmission electron microscopy (TEM). Figure 3 shows the effects of shear on the morphology of apoC-II amyloid fibrils. The images reveal that the morphologies of apoC-II fibrils formed at shear rates of 150 and 300 $s^{-1}$ are similar to those formed in the absence of a shear field, displaying a typical twisted-ribbon appearance as previously reported.[30] At a shear rate of 500 $s^{-1}$, the fibrils that are formed display a ropelike morphology indicating tangling and twisting of fibrils into thicker more aggregated structures.

**Shear-Induced Unfolding of ApoC-II.** The effects of shear on the secondary structure of apoC-II were examined at a low apoC-II concentration (50 $\mu$g/mL) where fibril formation is negligible.[47] The circular dichroism (CD) spectrum of monomeric apoC-II (Figure 4) is consistent with predominantly unordered structure with a characteristic minimum at 205 nm, similar to that previously reported.[30] The application of a shear field (500 $s^{-1}$) induced time-dependent changes in CD over a 5 min period, indicative of a loss of secondary structure. These changes were not reversed over a 5 min recovery period when the shear field was removed. Figure 4C summarizes the change in ellipticity at 205 nm during shear flow for 5 min and for the subsequent 5 min recovery period in the absence of shear. The results indicate an irreversible change in secondary structure after shear exposure.

Shear-induced changes in monomeric apoC-II W26 fluorescence were also observed. Figure 5 shows W26 emission spectra

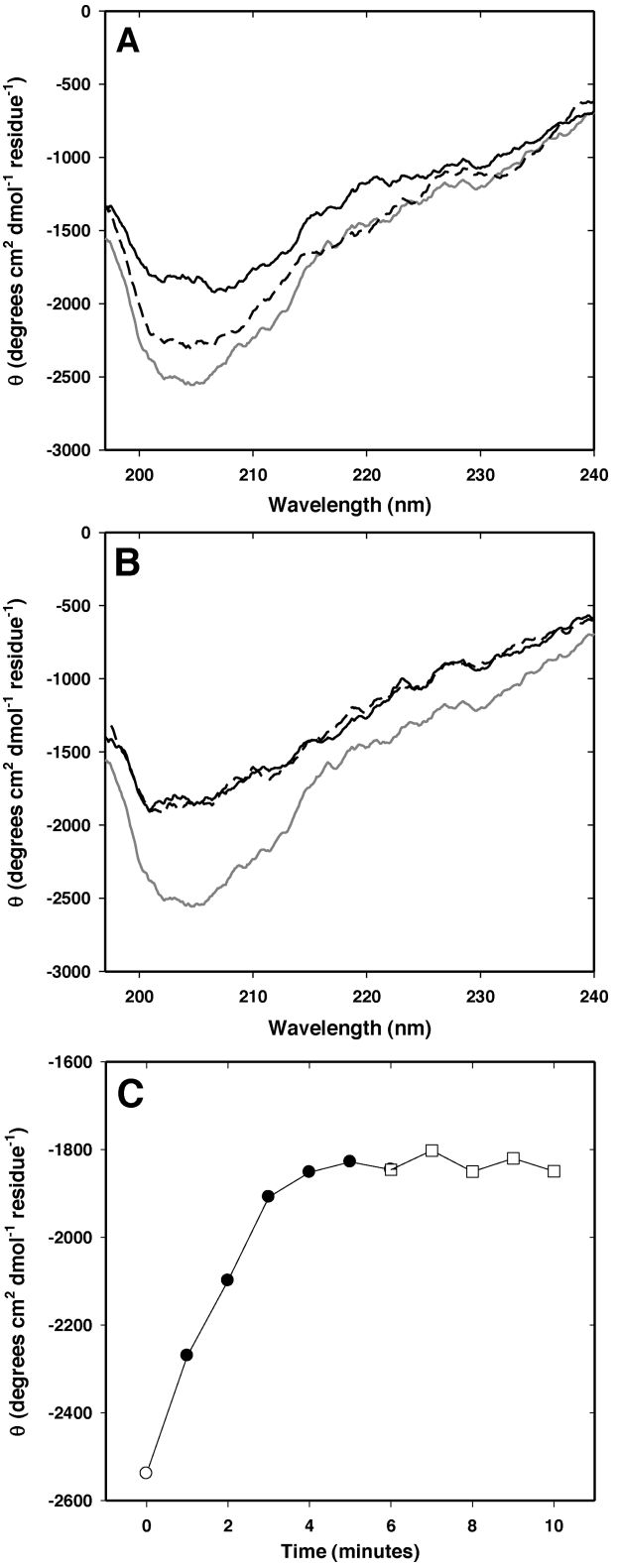


**Figure 4.** Circular dichroism (CD) spectra of apoC-II. CD spectra of freshly prepared apoC-II (50 $\mu$g/mL) were recorded (A) during shear (500 $s^{-1}$) and (B) after the shear field was stopped. Gray, solid lines (A and B) show identical CD spectra before shear ($t$ = 0 min). Black, dashed lines show CD spectra collected after 1 min [$t$ = 1 min (A), and $t$ = 6 min (B)]. Black, solid lines show CD spectra collected after 5 min [$t$ = 5 min (A), and $t$ = 10 min (B)]. (C) Changes in ellipticity at 205 nm before shear (○), during shearing (●), and after shear has been stopped (□).

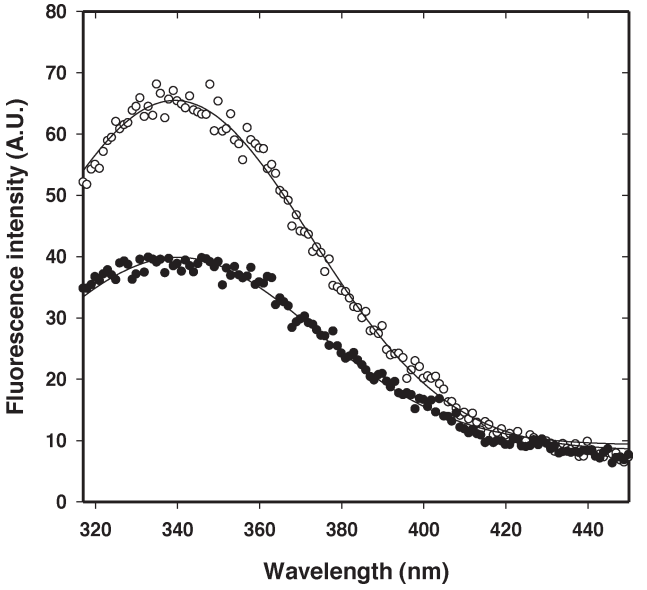


**Figure 5.** Effect of shear on the tryptophan emission of the apoC-II monomer. ApoC-II (50 $\mu$g/mL in refolding buffer) was freshly prepared. Emission spectra were recorded after excitation at 295 nm for freshly refolded samples prior to shear (○) and for samples after shear at 500 $s^{-1}$ for 30 min (●).

after excitation of W26 within apoC-$II_{S11C}$ monomers before ($t$ = 0 min) and after ($t$ = 30 min) the sample had been subjected to shear flow (500 $s^{-1}$). The observed decrease in W26 emission after shear flow indicates quenching as this residue becomes more exposed to the aqueous environment.

**FRET Analysis of the Effects of Shear Flow.** Cysteine-containing mutants were constructed (apoC-$II_{S11C}$, apoC-$II_{V45C}$, and apoC-$II_{W26F/Y37W/S61C}$) and modified with the 1,5-I-AEDANS fluorophore. These derivatives were used in FRET experiments, with the single tryptophan as the donor and the extrinsic AEDANS fluorophore as the acceptor. As FRET relies on the distance-dependent transfer of energy from a donor fluorophore to an acceptor fluorophore, this technique provides a spectroscopic ruler for measuring the distance between the two fluorophores during shear flow.

Figure 6 shows representative fluorescence data during shear flow (500 $s^{-1}$) for apoC-$II_{S11C}$ and apoC-$II_{S11C\text{-}AEDANS}$, presented as normalized fluorescence emission. For both samples, tryptophan fluorescence becomes quenched when shear flow commences (Figure 6A), consistent with the results presented in Figure 5. AEDANS fluorescence emission also decreases in a time-dependent manner during shear flow (Figure 6B). Figure 6C shows a shear-induced decrease in the extent of FRET upon excitation of tryptophan and monitoring AEDANS emission. The interpretation of this change is complex because the change could be due to a direct effect of shear flow on tryptophan or AEDANS fluorescence (Figure 6A) or due to a decrease in the extent of FRET from tryptophan to AEDANS. To resolve this uncertainty, FRET efficiencies were calculated from the tryptophan emission intensity for apoC-II derivatives with and without the AEDANS acceptor. FRET efficiencies were then determined before and after the samples had been subjected to shear flow (500 $s^{-1}$) for 30 min (Figure 6D). The results showed that shear flow reduces FRET efficiencies, indicating an increase in the distances between tryptophan and AEDANS for the three apoC-II


dx.doi.org/10.1021/bi2002482 |*Biochemistry* 2011, 50, 4046–4057

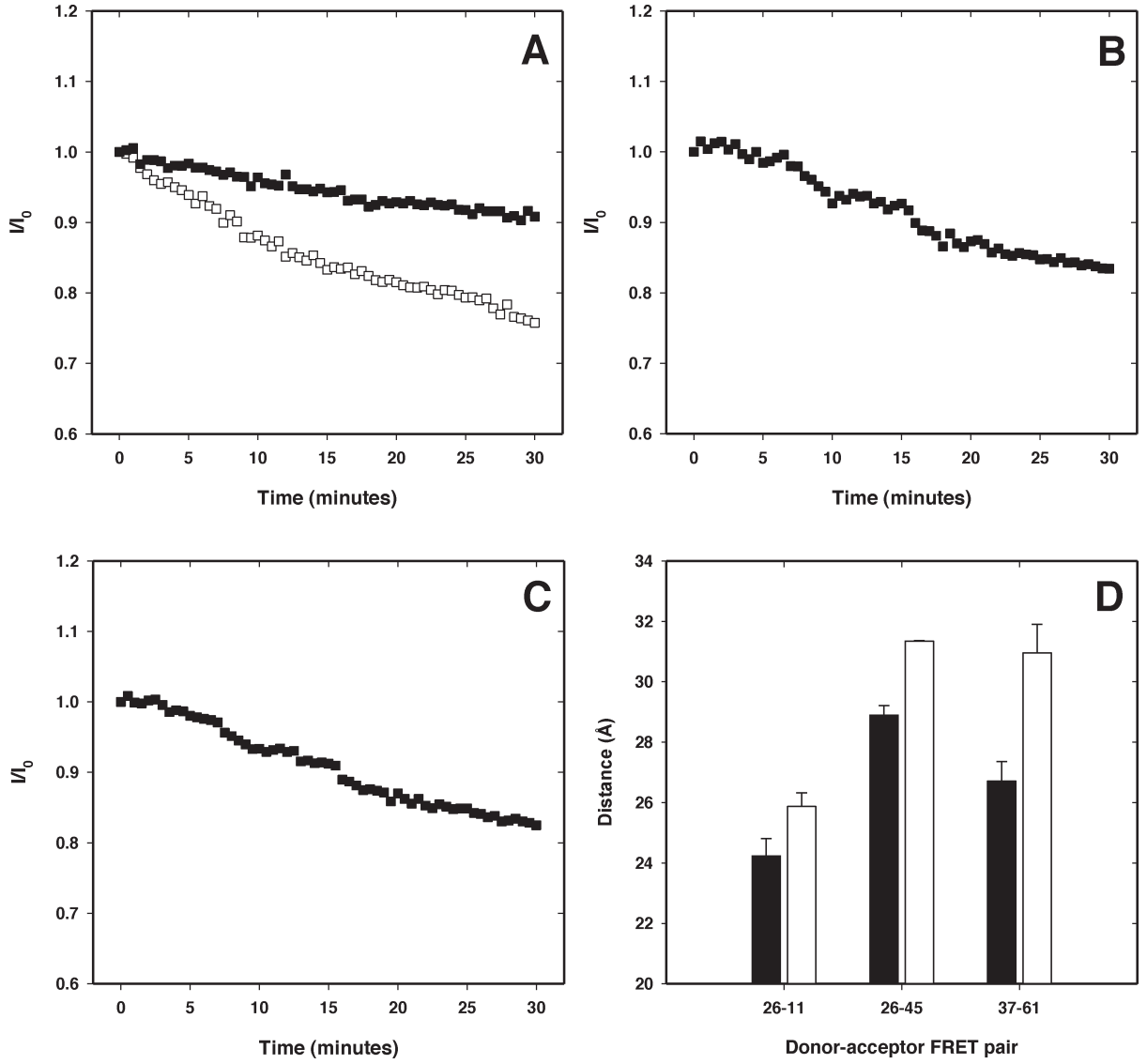


**Figure 6.** FRET analysis of the apoC-II monomer in the presence of shear. ApoC-II (50 $\mu$g/mL in refolding buffer) was freshly prepared and subjected to shear at 500 $s^{-1}$ for 30 min. (A−C) Relative real-time fluorescence changes for apoC-$II_{S11C}$ (□) and apoC-$II_{S11C\text{-}AEDANS}$ (■) in the presence of shear. (A) Trp fluorescence change, using an excitation wavelength of 295 nm and an emission wavelength of 350 nm. (B) AEDANS fluorescence change, using an excitation wavelength of 336 nm and an emission wavelength of 490 nm. (C) FRET signal change, using an excitation wavelength of 295 nm and an emission wavelength of 490 nm. (D) Distance between donor and acceptor based on FRET efficiencies calculated from Trp fluorescence change in the absence and presence of AEDANS, at 0 min (filled bars) and 30 min (empty bars). The error bars indicate standard deviations determined from duplicate measurements.

AEDANS derivatives examined. Together, these observations suggest that shear induces an irreversible conformational change where the donor and acceptor molecules become more exposed to the aqueous environment and, at the same time, move farther apart as the apoC-II molecule unfolds.

**Shear-Induced Formation of ApoC-II Oligomeric Intermediates.** Sedimentation velocity analysis was conducted using a high-sensitivity fluorescence detection system (FDS) and the analytical ultracentrifuge. Fluorescence intensity scans during sedimentation of Alexa488-labeled apoC-II samples (50 $\mu$g/mL) before and after exposure to shear flow are presented in Figure 7. The samples obtained after exposure to shear were diluted approximately 3-fold prior to analysis. The radial scans were analyzed assuming a $c(s)$ continuous distribution of sedimentation coefficients. The results for Alexa488-labeled apoC-II before exposure to shear indicate a single species with a modal sedimentation coefficient of approximately 1 S, consistent with monomeric apoC-II.[47] For Alexa488-labeled apoC-II subjected to a shear rate of 300 $s^{-1}$ for 30 min, two species with apparent sedimentation coefficients of 1 and 2.7 S were observed. A more abundant oligomeric species with an apparent sedimentation coefficient of 4 S was detected after exposure for 30 min at the higher shear rate of 500 $s^{-1}$.

**Seeding Experiment Using Shear-Induced ApoC-II Oligomeric Intermediates.** To determine if the shear-induced higher-order oligomeric species is an on-pathway intermediate for apoC-II fibril formation, aliquots of sheared protein were incubated with unsheared apoC-II under quiescent fibril-forming conditions. ApoC-II at a concentration where fibril formation is not detectable (50 $\mu$g/mL) was first sheared in Couette flow at

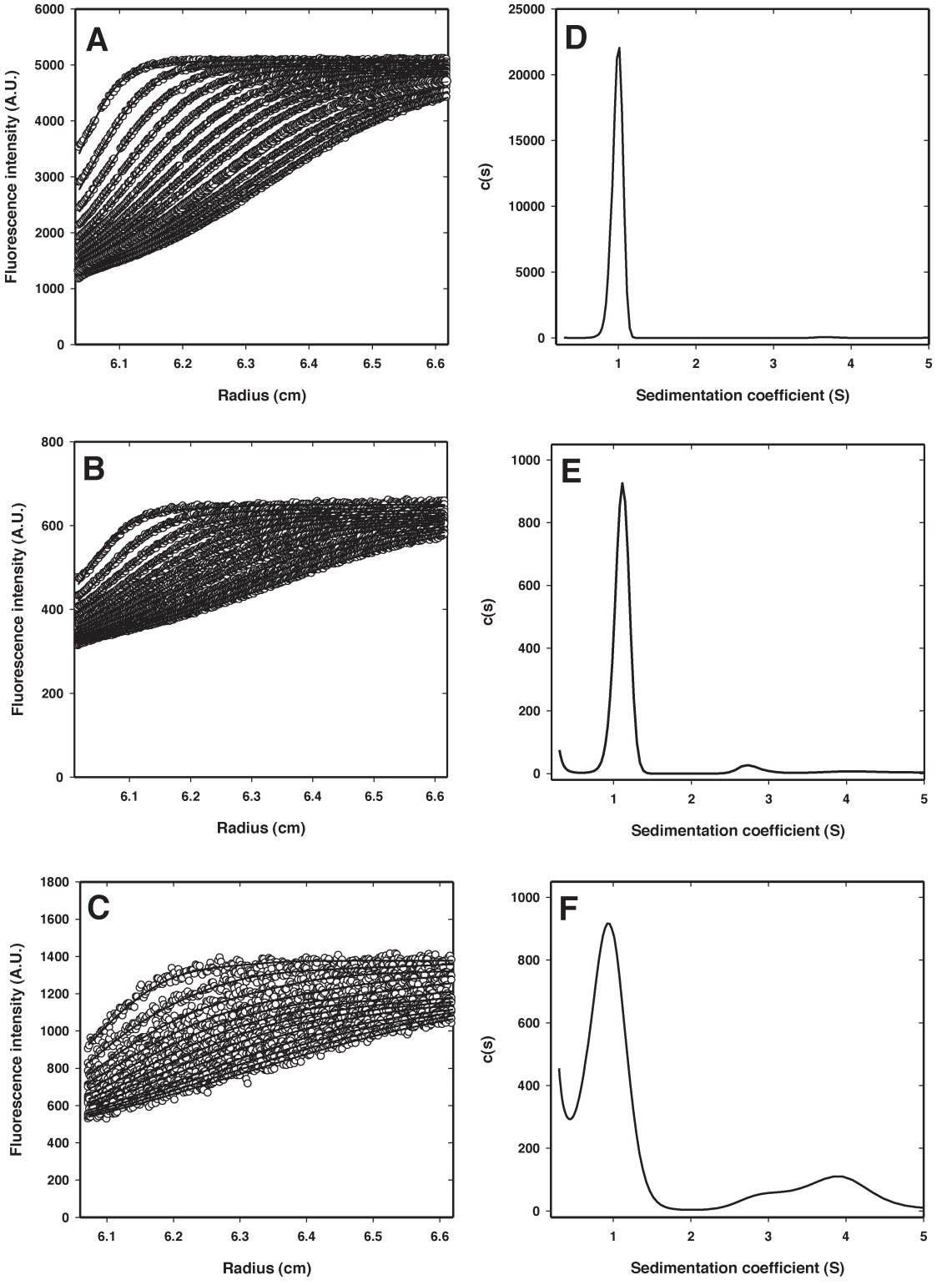


**Figure 7.** Sedimentation velocity data for freshly prepared Alexa488-labeled apoC-II (50 $\mu$g/mL) obtained using fluorescence detection in an analytical centrifuge. Shown are freshly prepared Alexa488-labeled apoC-II (50 $\mu$g/mL) without shear (A) and after being exposed for 30 min to shear rates of 300 (B) and 500 $s^{-1}$ (C) at room temperature. The samples obtained after exposure to shear were diluted approximately 3-fold prior to analysis in the ultracentrifuge. The data were obtained using an angular velocity of 50000 rpm (201600*g*). For the sake of clarity, only every eighth data scan is shown. The solid lines through the data in panels A–C were obtained by fitting the data to a continuous size distribution $c(s)$ model, yielding the corresponding distributions in panels D and E.

500 $s^{-1}$ for a period of 30 min and then retained for subsequent analysis. An equivalent solution without shear treatment was also retained as a control. ApoC-II solutions were freshly refolded in the absence and presence of sheared protein (3.5%, w/w) to a


dx.doi.org/10.1021/bi2002482 |*Biochemistry* 2011, 50, 4046–4057

final protein concentration of 0.3 mg/mL. The ThT fluorescence development of the samples was then monitored immediately after the initiation of fibril formation, at selected time points for more than 300 h until fibril formation was complete (Figure 8). When apoC-II fibrils were formed spontaneously without seeding, the $t_{50}$ value (19.5 h) is similar to that in the case in which fibrils are formed in the presence of unsheared seeds (20.5 h). In contrast, addition of sheared material accelerated the formation of fibrils by apoC-II, with a $t_{50}$ value of 16.8 h. This observation supports the hypothesis that the oligomeric species generated by shearing act to seed fibril formation and are therefore on-pathway intermediates in apoC-II fibril formation.

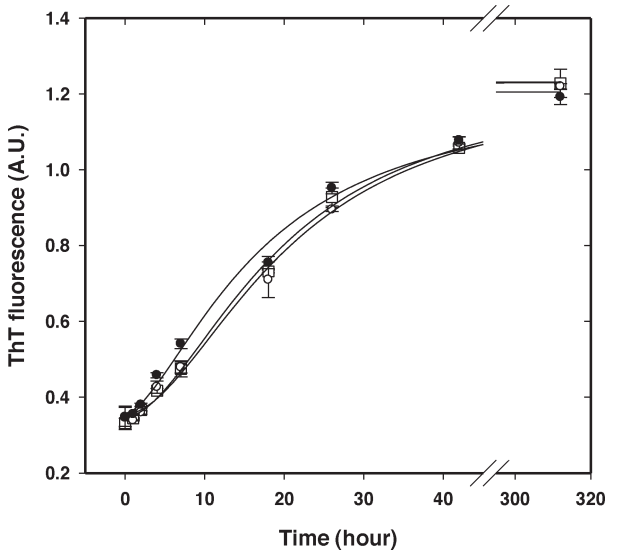


**Figure 8.** Seeding of apoC-II fibril formation by preformed shear-induced higher-order species. Freshly refolded apoC-II (50 $\mu$g/mL) sheared in Couette flow for 30 min at 500 $s^{-1}$ was retained and used as seed. Formation of fibrils by apoC-II at a final concentration of 0.3 mg/mL was induced in the presence of sheared (●) and unsheared (gray circles) seeds at 3.5% (w/w), as well as in the absence of seeds (□) as controls. The ThT fluorescence development of the samples was monitored.

## DISCUSSION

Given that protein conformation is critical to its function, studies of the shear stability of dilute protein systems have significant implications for much of biology. Although there has been progress in investigating the influence of shear flow on protein aggregation, conflicting reports abound in the literature because of the use of indirect experimental evidence in explaining this phenomenon.[38,40,42,43] With the advent of sensitive optical techniques, increasingly direct measurements of the conformational dynamics of protein molecules in controlled flow fields, e.g., Couette flow, are now available.[44−46,48,55,56] The current observation that shear flow enhances apoC-II fibril formation is consistent with our previous reports showing shear-induced fibril formation by $\beta$-lactoglobulin[46] and effects of shear on protein aggregation using amyloid-$\beta$ as a model system.[49] The observations presented here suggest that the fluid drag in the flow field induces a structural rearrangement of the predominantly random coil apoC-II monomers, leading to their rapid polymerization into $\beta$-sheet-rich fibrillar aggregates. To explain these observations, we find it is important to appreciate the nature of the flow field employed.

Simple shear flow is considered as a superposition of rotational and extensional forces around the vorticity axis.[57] ApoC-II monomers exposed to a simple Couette flow are exposed to both extensive and compressive hydrodynamic forces during this cycle as a result of the velocity gradient experienced by the molecule. We assume that it is the orientation relative to the flow field where the extensional forces act that causes stretching and unfolding to occur.[45] Kuhn predicted that maximal chain stretching occurs when a polymer, modeled as a dumbbell of two beads on a spring, makes an angle of 45° with the direction of flow in the flow field.[58] The maximal extensive force experienced by a given molecule in a solvent with a constant viscosity is directly proportional to the shear rate.[58] The results show that fluid forces in simple shear flow perturb the native conformation of apoC-II monomers, leading to an irreversible structural change (Figures 4 and 5). The FRET studies (Figure 6) show that this conformational change involves the stretching of apoC-II monomers in the flow field, which potentially leads to the evolution of solvent-exposed hydrophobic segments, initially concealed from

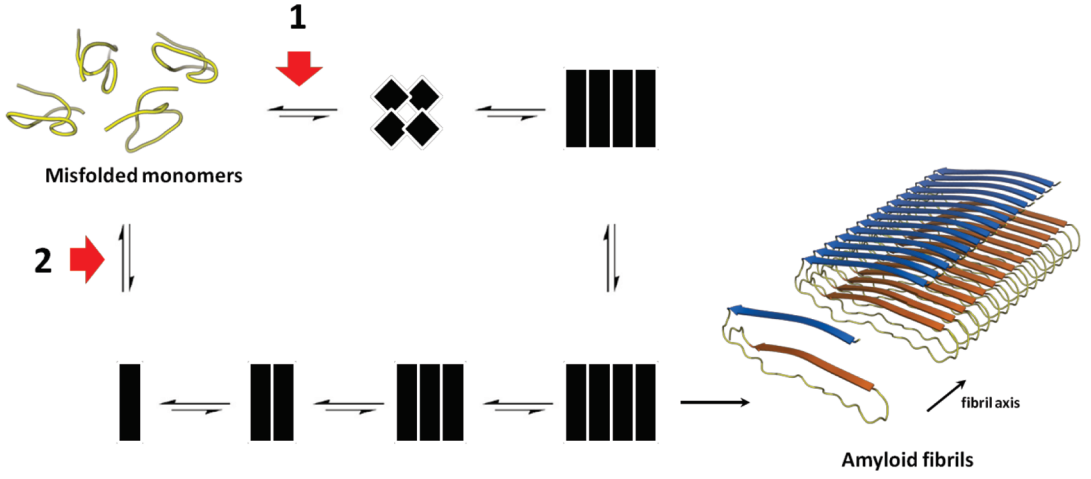


**Figure 9.** Proposed model of apoC-II amyloid fibril assembly. Pathway 1 proposes a rate-determining formation of a tetrameric intermediate based on previous studies of lipid-induced acceleration of fibril formation.[47] Pathway 2 proposes a rate-determining isomerization of misfolded monomers to form an amyloidogenic monomeric species. The thick arrows indicate proposed steps accelerated by shear.

the aqueous environment, as well as other bonding sites facilitating intermolecular interactions. It is thus not surprising that the shear exposure triggers the evolution of prefibrillar oligomeric aggregates (Figure 7), resulting from the intermolecular association of unfolded monomers, primarily if not entirely via hydrophobic interactions. The seeding experiments showed that these aggregates are on-pathway species acting to nucleate fibril assembly in apoC-II solutions, thereby reducing the time required for fibril development (Figure 8). The observed shear effect was more pronounced with an increasing shear rate (Figure 1), which attests to the increased fluid drag, hence rapid stretching (unfolding) of apoC-II monomers, in the flow field, accelerating aggregation.

Variations in the morphology of fibrillar aggregates were observed depending on the magnitude of the shear rate applied (Figure 3), which has been previously observed for $\beta$-lactoglobulin.[59] Whereas fibrils formed at relatively low shear rates displayed an even distribution of the typical twisted-ribbon-like appearance, fibrils formed at high shear rates displayed a ropelike structure. It has been proposed that polymers in simple shear flow experience temporal fluctuations that involve periodic elongation, relaxation, and tumbling.[57,60] Considering that a relatively high concentration of apoC-II (1 mg/mL) was used in this study, the possibility of tangling of partially extended monomers, during the periodic end-over-end tumbling in the flow field, may result in the decreased rate of apoC-II fibril formation at 500 $s^{-1}$, as well as the intertwining of several individual fibrils into the ropelike structures.

Figure 9 summarizes possible pathways for apoC-II amyloid fibril formation. Pathway 1 of the model involves the rate-determining formation of a tetrameric species that nucleates fibril formation. These steps are based on previous studies that show that the lipid-induced acceleration of apoC-II fibril formation involves the formation of a stable tetramer.[47] The alternative mechanism (pathway 2) proposes a rate-determining isomerization of misfolded monomers to generate a species that rapidly assembles into mature fibrils. Evidence of this pathway is provided by studies of cross-linked apoC-II dimers, which act as seeds to rapidly accelerate apoC-II fibril formation.[61] The ability of small amounts of sheared apoC-II samples to seed apoC-II fibril formation (Figure 8) provides direct evidence that shear promotes the irreversible formation of intermediates in the fibril formation pathway. We propose that the fluid forces associated with shear flow induce an irreversible conformational change in native apoC-II monomers. These partially extended conformations may rapidly coalesce into prefibrillar aggregates (pathway 1). Alternatively, shear forces may promote a pathway that drives isomerization of monomeric apoC-II into a conformation that favors the rapid self-assembly of apoC-II isomers into mature fibrils. As illustrated in Figure 9, shear flow could accelerate fibril development by acting on pathway 1 or 2. These mechanisms may be general for other amyloidogenic proteins.[48] An additional and complementary mechanism for the shear-induced formation of amyloid fibrils must also be considered. Theoretical modeling studies predict an increase in the level of fibril fragmentation should increase the concentration of growing fibrils leading to significantly increased rates of fibril formation.[62,63] This prediction is supported by recent studies showing laser-induced acceleration of A$\beta$ amyloid fibril formation.[64] Shear-induced fragmentation of $\beta$2-microglobulin fibrils leading to an increase in fibril toxicity[65] suggests that shear forces may act in multiple ways to affect the rate of formation and properties of amyloid fibrils.

The shear rates experienced in vivo vary over a wide range. Arterial wall shear rates are estimated to range between 135 and 1700 $s^{-1}$,[66] while in partly clogged arterioles, hemodynamic shear rates approach $10^4$ $s^{-1}$.[67] In addition, protein molecules experience a high level of confinement under physiological flow in capillaries and in the filtering organs. Others have shown that molecular confinement accelerates the deformation of entangled polymers under squeeze flow[68] under conditions comparable to those associated with blood flow. Therefore, though the shear rates investigated in this study are within the physiological range,[66] the Couette shear exposure is less complex than that to which the protein is exposed in blood flow. In this sense, this study shows the effect of the true simple shear flow on protein conformation and aggregation. Nonetheless, this information might help explain the mechanism of shear-induced protein deformation and consequent plaque deposition in vivo. Amyloid has not been identified in blood but is deposited in proximal tissue, e.g., vessel walls.[69,70] Shear flow may form oligomeric precursors in blood that are subsequently taken up in tissue where they nucleate fibrillogenesis. Furthermore, the propagation of amyloid diseases may be promoted by shear degradation of fibrils to generate new seeds, which can be transported to new deposition sites by fluid flow. Clinical examples of amyloidoses associated with fluid flow include the incidence of hemodialysis-related amyloidoses in patients with renal failure.[71] Although the causal relationship needs to be established, the ability of shear to facilitate amyloid formation has significant implications for the onset of protein conformational disorders.

In conclusion, we have shown that shear accelerated the rate of formation of apoC-II fibrils. Evidence of the stretching of apoC-II monomers in the flow field leading to an irreversible structural change and exposure of the initially solvent-concealed hydrophobic segments and intermolecular bonding sites is presented. Intermolecular association of denatured monomers gives rise to on-pathway prefibrillar oligomeric species, which nucleate apoC-II fibril assembly and reduce the time required for fibril development.

## AUTHOR INFORMATION

### Corresponding Author

*Department of Chemical and Biomolecular Engineering, The University of Melbourne, Parkville, Victoria 3010, Australia. Telephone: 61-3-8344 8261. Fax: 61-3-8344 4153. E-mail: davided@unimelb.edu.au.

### Funding Sources

This research was supported by the Australian Research Council (DP0877800).

## ACKNOWLEDGMENT

We thank Dr. Victoria Hughes for her assistance with fluorescence and CD spectroscopy and Dr. Ken Goldie for his assistance with the TEM.

## ABBREVIATIONS

apo, apolipoprotein; CD, circular dichroism; FDS, fluorescence detection system; FRET, fluorescence resonance energy transfer; GuHCl, guanidine hydrochloride; 1,5-I-AEDANS, 5-({2-[(iodoacetyl)amino]ethyl}amino)naphthalene-1-sulfonic acid; PLL, poly-L-lysine; SAP, serum amyloid P; TEM, transmission electron microscopy; ThT, thioflavin T; vWF, von Willebrand factor.

## REFERENCES


(1) Sipe, J. D., and Cohen, A. S. (2000) Review: History of the amyloid fibril. *J. Struct. Biol. 130*, 88–98.

(2) Chiti, F., and Dobson, C. M. (2006) Protein misfolding, functional amyloid, and human disease. *Annu. Rev. Biochem. 75*, 333–366.

(3) Dobson, C. M. (2003) Protein folding and misfolding. *Nature 426*, 884–890.

(4) Dobson, C. M. (2002) Getting out of shape. *Nature 418*, 729–730.

(5) Uversky, V. N., Li, J., and Fink, A. L. (2001) Evidence for a partially folded intermediate in α-synuclein fibril formation. *J. Biol. Chem. 276*, 10737–10744.

(6) Ahmad, A., Millett, I. S., Doniach, S., Uversky, V. N., and Fink, A. L. (2003) Partially folded intermediates in insulin fibrillation. *Biochemistry 42*, 11404–11416.

(7) Alexandrescu, A. T. (2005) Amyloid accomplices and enforcers. *Protein Sci. 14*, 1–12.

(8) Azuaga, A. I., Dobson, C. M., Mateo, P. L., and Conejero-Lara, F. (2002) Unfolding and aggregation during the thermal denaturation of streptokinase. *Eur. J. Biochem. 269*, 4121–4133.

(9) Gosal, W. S., Morten, I. J., Hewitt, E. W., Smith, D. A., Thomson, N. H., and Radford, S. E. (2005) Competing pathways determine fibril morphology in the self-assembly of β2-microglobulin into amyloid. *J. Mol. Biol. 351*, 850–864.

(10) Giri, K., Bhattacharyya, N. P., and Basak, S. (2007) pH-dependent self-assembly of polyalanine peptides. *Biophys. J. 92*, 293–302.

(11) Carneiro, F. A., Ferradosa, A. S., and Da Poian, A. T. (2001) Low pH-induced conformational changes in vesicular stomatitis virus glycoprotein involve dramatic structure reorganization. *J. Biol. Chem. 276*, 62–67.

(12) Zhao, H., Tuominen, E. K., and Kinnunen, P. K. (2004) Formation of amyloid fibers triggered by phosphatidylserine-containing membranes. *Biochemistry 43*, 10302–10307.

(13) Griffin, M. D., Mok, M. L., Wilson, L. M., Pham, C. L., Waddington, L. J., Perugini, M. A., and Howlett, G. J. (2008) Phospholipid interaction induces molecular-level polymorphism in apolipoprotein C-II amyloid fibrils via alternative assembly pathways. *J. Mol. Biol. 375*, 240–256.

(14) Stewart, C. R., Tseng, A. A., Mok, Y. F., Staples, M. K., Schiesser, C. H., Lawrence, L. J., Varghese, J. N., Moore, K. J., and Howlett, G. J. (2005) Oxidation of low-density lipoproteins induces amyloid-like structures that are recognized by macrophages. *Biochemistry 44*, 9108–9116.

(15) Binger, K. J., Griffin, M. D., and Howlett, G. J. (2008) Methionine oxidation inhibits assembly and promotes disassembly of apolipoprotein C-II amyloid fibrils. *Biochemistry 47*, 10208–10217.

(16) Wong, Y. Q., Binger, K. J., Howlett, G. J., and Griffin, M. D. (2010) Methionine oxidation induces amyloid fibril formation by full-length apolipoprotein A-I. *Proc. Natl. Acad. Sci. U.S.A. 107*, 1977–1982.

(17) Collins, S. R., Douglass, A., Vale, R. D., and Weissman, J. S. (2004)Mechanism of prion propagation: Amyloid growth occurs by monomer addition. *PLoS Biol. 2*, e321.

(18) Liu, J. J., and Lindquist, S. (1999) Oligopeptide-repeat expansions modulate 'protein-only' inheritance in yeast. *Nature 400*, 573–576.

(19) Serio, T. R., Cashikar, A. G., Kowal, A. S., Sawicki, G. J., Moslehi, J. J., Serpell, L., Arnsdorf, M. F., and Lindquist, S. L. (2000) Nucleated conformational conversion and the replication of conformational information by a prion determinant. *Science 289*, 1317.

(20) Ohhashi, Y., Kihara, M., Naiki, H., and Goto, Y. (2005) Ultrasonication-induced amyloid fibril formation of β2-microglobulin. *J. Biol. Chem. 280*, 32843–32848.

(21) Maruyama, T., Katoh, S., Nakajima, M., and Nabetani, H. (2001) Mechanism of bovine serum albumin aggregation during ultrafiltration. *Biotechnol. Bioeng. 75*, 233–238.

(22) Moore, R. A., Hayes, S. F., Fischer, E. R., and Priola, S. A. (2007) Amyloid formation via supramolecular peptide assemblies. *Biochemistry 46*, 7079–7087.

(23) Petkova, A. T., Leapman, R. D., Guo, Z., Yau, W. M., Mattson, M. P., and Tycko, R. (2005) Self-propagating, molecular-level polymorphism in Alzheimer's β-amyloid fibrils. *Science 307*, 262–265.

(24) Stehbens, W. E. (1979) *Hemodynamics and the blood vessel wall*, Charles C. Thomas Publishing, Springfield, IL.

(25) Mucchiano, G. I., Haggqvist, B., Sletten, K., and Westermark, P. (2001)Apolipoprotein A-1-derived amyloid in atherosclerotic plaques of the human aorta. *J. Pathol. 193*, 270–275.

(26) Rocken, C., Tautenhahn, J., Buhling, F., Sachwitz, D., Vockler, S., Goette, A., and Burger, T. (2006) Prevalence and pathology of amyloid in atherosclerotic arteries. *Arterioscler., Thromb., Vasc. Biol. 26*, 676–677.

(27) Howlett, G. J., and Moore, K. J. (2006) Untangling the role of amyloid in atherosclerosis. *Curr. Opin. Lipidol. 17*, 541–547.

(28) Hatters, D. M., and Howlett, G. J. (2002) The structural basis for amyloid formation by plasma apolipoproteins: A review. *Eur. Biophys. J. 31*, 2–8.

(29) Teoh, C. L., Griffin, M. D. W., and Howlett, G. J. (2011) Apolipoproteins and amyloid fibril formation in atherosclerosis. *Protein Cell 2*, 116–127.

(30) Hatters, D. M., MacPhee, C. E., Lawrence, L. J., Sawyer, W. H., and Howlett, G. J. (2000) Human apolipoprotein C-II forms twisted amyloid ribbons and closed loops. *Biochemistry 39*, 8276–8283.

(31) Hatters, D. M., MacRaild, C. A., Daniels, R., Gosal, W. S., Thomson, N. H., Jones, J. A., Davis, J. J., MacPhee, C. E., Dobson, C. M., and Howlett, G. J. (2003) The circularization of amyloid fibrils formed by apolipoprotein C-II. *Biophys. J. 85*, 3979–3990.

(32) Teoh, C. L., Pham, C. L., Todorova, N., Hung, A., Lincoln, C. N., Lees, E., Lam, Y. H., Binger, K. J., Thomson, N. H., Radford, S. E., Smith, T. A., Muller, S. A., Engel, A., Griffin, M. D., Yarovsky, I., Gooley, P. R., and Howlett, G. J. (2011) A structural model for apolipoprotein C-II amyloid fibrils: Experimental characterization and molecular dynamics simulations. *J. Mol. Biol. 405*, 1246–1266.

(33) MacRaild, C. A., Stewart, C. R., Mok, Y. F., Gunzburg, M. J., Perugini, M. A., Lawrence, L. J., Tirtaatmadja, V., Cooper-White, J. J., and Howlett, G. J. (2004) Non-fibrillar components of amyloid deposits mediate the self-association and tangling of amyloid fibrils. *J. Biol. Chem. 279*, 21038–21045.

(34) Gunzburg, M. J., Perugini, M. A., and Howlett, G. J. (2007) Structural basis for the recognition and cross-linking of amyloid fibrils by human apolipoprotein E. *J. Biol. Chem. 282*, 35831–35841.

(35) Stewart, C. R., Haw, A., III, Lopez, R., McDonald, T. O., Callaghan, J. M., McConville, M. J., Moore, K. J., Howlett, G. J., and O'Brien, K. D. (2007) Serum amyloid P colocalizes with apolipoproteins in human atheroma: Functional implications. *J. Lipid Res. 48*, 2162–2171.

(36) Medeiros, L. A., Khan, T., El Khoury, J. B., Pham, C. L., Hatters, D. M., Howlett, G. J., Lopez, R., O'Brien, K. D., and Moore, K. J. (2004) Fibrillar amyloid protein present in atheroma activates CD36 signal transduction. *J. Biol. Chem. 279*, 10643–10648.

(37) Astbury, W. T., and Woods, H. J. (1934) X-ray studies of the structure of hair, wool, and related fibres. II. The molecular structure and elastic properties of hair keratin. *Philos. Trans. R. Soc. London, Ser. A 232*, 333–394.

(38) Charm, S. E., and Wong, B. L. (1970) Enzyme inactivation with shearing. *Biotechnol. Bioeng. 12*, 1103–1109.

(39) De Gennes, P. G. (1974) Coil-stretch transition of dilute flexible polymers under ultrahigh velocity gradients. *J. Chem. Phys. 60*, 5030–5042.

(40) Jaspe, J., and Hagen, S. J. (2006) Do protein molecules unfold in a simple shear flow? *Biophys. J. 91*, 3415–3424.

(41) Szymczak, P., and Cieplak, M. (2006) Stretching of proteins in a uniform flow. *J. Chem. Phys. 125*, 164903.

(42) Thomas, C. R., and Dunnill, P. (1979) Action of shear on enzymes: Studies with catalase and urease. *Biotechnol. Bioeng. 21*, 2279–2302.

(43) Schneider, S. W., Nuschele, S., Wixforth, A., Gorzelanny, C., Alexander-Katz, A., Netz, R. R., and Schneider, M. F. (2007) Shear-induced unfolding triggers adhesion of von Willebrand factor fibers. *Proc. Natl. Acad. Sci. U.S.A. 104*, 7899–7903.

(44) Lee, A. T., and McHugh, A. J. (1999) The effect of simple shear flow on the helix-coil transition of poly-L-lysine. *Biopolymers 50*, 589–594.

(45) Bekard, I. B., Barnham, K. J., White, L. R., and Dunstan, D. E. (2011) α-Helix unfolding in simple shear flow. *Soft Matter 7*, 203–210.
(46) Hill, E. K., Krebs, B., Goodall, D. G., Howlett, G. J., and Dunstan, D. E. (2006) Shear flow induces amyloid fibril formation. *Biomacromolecules 7*, 10–13.
(47) Ryan, T. M., Howlett, G. J., and Bailey, M. F. (2008) Fluorescence detection of a lipid-induced tetrameric intermediate in amyloid fibril formation by apolipoprotein C-II. *J. Biol. Chem. 283*, 35118–35128.
(48) Bekard, I. B., and Dunstan, D. E. (2009) Shear-induced deformation of bovine insulin in Couette flow. *J. Phys. Chem. B 113*, 8453–8457.
(49) Hamilton-Brown, P., Bekard, I., Ducker, W. A., and Dunstan, D. E. (2008)How does shear affect Aβ fibrillogenesis? *J. Phys. Chem. B 112*, 16249–16252.
(50) Hatters, D. M., Minton, A. P., and Howlett, G. J. (2002) Macromolecular crowding accelerates amyloid formation by human apolipoprotein C-II. *J. Biol. Chem. 277*, 7824–7830.
(51) Wu, P., and Brand, L. (1994) Resonance energy transfer: Methods and applications. *Anal. Biochem. 218*, 1–13.
(52) MacGregor, I. K., Anderson, A. L., and Laue, T. M. (2004) Fluorescence detection for the XLI analytical ultracentrifuge. *Biophys. Chem. 108*, 165–185.
(53) Mok, Y. F., Ryan, T. M., Yang, S., Hatters, D. M., Howlett, G. J., and Griffin, M. D. (2010) Sedimentation velocity analysis of amyloid oligomers and fibrils using fluorescence detection. *Methods*.
(54) Schuck, P. (2003) On the analysis of protein self-association by sedimentation velocity analytical ultracentrifugation. *Anal. Biochem. 320*, 104–124.
(55) Dunstan, D. E., Hamilton-Brown, P., Asimakis, P., Ducker, W., and Bertolini, J. (2009) Shear flow promotes amyloid-β fibrilization. *Protein Eng., Des. Sel. 22*, 741–746.
(56) Singh, I., Themistou, E., Porcar, L., and Neelamegham, S. (2009) Fluid Shear Induces Conformation Change in Human Blood Protein von Willebrand Factor in Solution. *Biophys. J. 96*, 2313–2320.
(57) Smith, D. E., Babcock, H. P., and Chu, S. (1999) Single-polymer dynamics in steady shear flow. *Science 283*, 1724–1727.
(58) Kuhn, W. (1933) Über quantitative deutung der viskosität und strömungsdoppelbrechung von suspensionen. *Kolloid-Z. 62*, 269–285.
(59) Dunstan, D. E., Hamilton-Brown, P., Asimakis, P., Ducker, W., and Bertolini, J. (2009) Shear-induced structure and mechanics of β-lactoglobulin amyloid fibrils. *Soft Matter 5*, 5020–5028.
(60) Alexander-Katz, A., Schneider, M. F., Schneider, S. W., Wixforth, A., and Netz, R. R. (2006) Shear-flow-induced unfolding of polymeric globules. *Phys. Rev. Lett. 97*, 138101.
(61) Pham, C. L., Hatters, D. M., Lawrence, L. J., and Howlett, G. J. (2002) Cross-linking and amyloid formation by N- and C-terminal cysteine derivatives of human apolipoprotein C-II. *Biochemistry 41*, 14313–14322.
(62) Knowles, T. P., Waudby, C. A., Devlin, G. L., Cohen, S. I., Aguzzi, A., Vendruscolo, M., Terentjev, E. M., Welland, M. E., and Dobson, C. M. (2009) An analytical solution to the kinetics of breakable filament assembly. *Science 326*, 1533–1537.
(63) Hall, D., and Edskes, H. (2009) A model of amyloid's role in disease based on fibril fracture. *Biophys. Chem. 145*, 17–28.
(64) Yagi, H., Ozawa, D., Sakurai, K., Kawakami, T., Kuyama, H., Nishimura, O., Shimanouchi, T., Kuboi, R., Naiki, H., and Goto, Y. (2010) Laser-induced propagation and destruction of amyloid beta fibrils. *J. Biol. Chem. 285*, 19660–19667.
(65) Xue, W. F., Hellewell, A. L., Gosal, W. S., Homans, S. W., Hewitt, E. W., and Radford, S. E. (2009) Fibril fragmentation enhances amyloid cytotoxicity. *J. Biol. Chem. 284*, 34272–34282.
(66) Stroev, P. V., Hoskins, P. R., and Easson, W. J. (2007) Distribution of wall shear rate throughout the arterial tree: A case study. *Atherosclerosis 191*, 276–280.
(67) Kroll, M. H., Hellums, J. D., McIntire, L. V., Schafer, A. I., and Moake, J. L. (1996) Platelets and shear stress. *Blood 88*, 1525–1541.
(68) Rowland, H. D., King, W. P., Pethica, J. B., and Cross, G. L. (2008) Molecular confinement accelerates deformation of entangled polymers during squeeze flow. *Science 322*, 720–724.
(69) Haggqvist, B., Naslund, J., Sletten, K., Westermark, G. T., Mucchiano, G., Tjernberg, L. O., Nordstedt, C., Engstrom, U., and Westermark, P. (1999) Medin: An integral fragment of aortic smooth muscle cell-produced lactadherin forms the most common human amyloid. *Proc. Natl. Acad. Sci. U.S.A. 96*, 8669–8674.
(70) Mucchiano, G., Cornwell, G. G., III, and Westermark, P. (1992) Senile aortic amyloid. Evidence for two distinct forms of localized deposits. *Am. J. Pathol. 140*, 871–877.
(71) Floege, J., and Ehlerding, G. (1996) β-2-Microglobulin-associated amyloidosis. *Nephron 72*, 9–26.